Template-Free Hierarchical Self-Assembly of a Pyrene Derivative into Supramolecular Nanorods

ChemComm

Accepted Manuscript

ROYAL SOCIETY OF CHEMISTRY

rsc.li/chemcomm

View Article Online
DOI: 10.1039/C6CC09731F

Chemical Communications

COMMUNICATION

Template-Free Hierarchical Self-Assembly of a Pyrene Derivative into Supramolecular Nanorods

Received 00th January 20xx,
Accepted 00th January 20xx

DOI: 10.1039/x0xx00000x

www.rsc.org/

Mohamed El Idrissi,[a] Simon J. Teat,[b] Philippe F-X. Corvini,[a] Martin J. Paterson,[c] Scott J. Dalgarno[c]* and Patrick Shahgaldian[a]*

The accurate molecular design of organic building blocks is of great importance for the creation of large supramolecular entities with precise dimensional organisation. Herein we report on the design of a new pyrene derivative that yields, through a hierarchical self-assembly process and in the absence of template, stable and well defined nanorods. X-ray diffraction studies allowed elucidation of the three dimensional packing of this pyrene derivative within the self-assembled nanorods.

One of the main challenges in supramolecular chemistry is the design of large self-assembled and functional nanomaterials, with precise control over the positioning of the constitutive building blocks in three dimensions. Hierarchical self-assembly is defined as the assembly of molecular building blocks into supramolecular structures of increasing order and complexity.[1] In this context, Nature represents a great source of inspiration as biology provides countless examples of elegant hierarchically assembled structures. One good example that substantiates this statement is the folding of linear polypeptides, which form secondary structures (α-helix, β-sheet) that, in turn, self-organise to yield more complex and functional tertiary and quaternary structures of functional proteins.

Although chemists can exploit a variety of non-covalent interactions to invoke the self-assembly of molecular building blocks into complex supramolecular structures,[2] stable and directional interactions are preferred as they allow for a better control over the self-assembly process. In this context, π-π stacking is of high significance as, besides a relatively high energy of interaction (ca. 10-70 kJ mol^{-1}),[3] it is highly directional. Consequently, π-π stacking has been largely exploited to produce one-dimensional nanostructures such as nanowires,[4] nanotubes,[5] or nanorods.[6,7]

When one considers the vast array of building blocks capable of self-assembling through π-π stacking, peptides,[8] porphyrins[9,10] and pyrene derivatives[11-13] have attracted special interest. The range of available functionalised pyrene derivatives, their self-assembly behaviour, as well as their remarkable optical and electronic properties render these chromophores ideal candidates for several applications, in particular those where control of molecular assembly into a defined structure is of high importance.[14] Although pyrene derivatives have been studied for their ability to form supramolecular nanorods, the self-assembly process typically requires the use of templates to yield well-defined structures.[15-19] Herein, we report the synthesis and template-free hierarchical self-assembly of a novel pyrene derivative into well-defined nanorods studied by means of fluorescence and UV-Vis spectroscopy, scanning electron microscopy, single crystal and powder X-ray diffraction studies.

The new pyrene derivative *N*-(3-(triethoxysilane)propyl)pyrene butylamide **1** was designed so as to possess the following features: i) the ability to form intermolecular π-π stacking interactions, ii) a complementary H-bond donor and acceptor group (i.e. amide) that provides additional control over the self-assembly process, and iii) the presence of bulky chemical functions (triethoxysilyl) that may be further exploited to functionalise the resulting self-assembled nanostructures (Scheme 1).

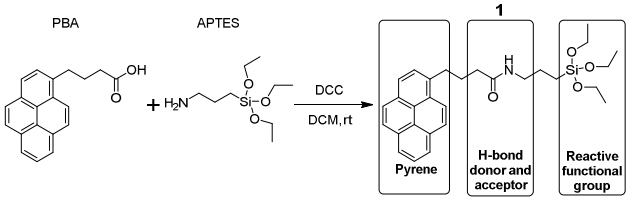

Scheme 1. Synthetic route to pyrene derivative **1**, highlighting the key structural features incorporated.

[a] *School of Life Sciences, University of Applied Sciences and Arts Northwestern Switzerland, Gründenstrasse 40, Muttenz CH-4132, Switzerland. Email: patrick.shahgaldian@fhnw.ch*
[b] *Advanced Light Source, Lawrence Berkeley National Laboratory Berkeley, CA 94720, USA.*
[c] *Institute of Chemical Science, Heriot-Watt University, Riccarton, Edinburgh, Scotland EH14 4AS UK. Email: S.J.Dalgarno@hw.ac.uk*
The Advanced Light Source is supported by the Director, Office of Science, Office of Basic Energy Sciences, of the US Department of Energy under contract No. DE-AC02-05CH11231.
Electronic Supplementary Information (ESI) available: See
DOI: 10.1039/x0xx00000x

View Article Online
DOI: 10.1039/C6CC09731F

Compound **1** was produced by activation of pyrene butyric acid with N,N'-dicyclohexylcarbodiimide and further reacted with 3-aminopropyl triethoxysilane (ESI Fig. S1-S3). While **1** was found to be readily soluble in ethanol, the addition of water rapidly caused formation of a stable milky white suspension. We used UV-Vis absorption spectroscopy to assess the self-assembly properties of **1**, taking advantage of its characteristic chromogenic properties. Spectra of **1** were first recorded in ethanol; analysis revealed well-resolved vibronic bands in the 250-370 nm range with four main peaks at 264, 274, 326 and 340 nm (Fig. 1). The ratio of the intensities of the vibronic bands at 326 and 340 nm, $I_{326/340}$, was measured to be 1.33.

A solution of **1** in ethanol was then poured into water (vol. water:ethanol, 90:10) and the vibronic bands were found to undergo a bathochromic shift; the bands at 264, 274, 326 and 340 nm were red-shifted to 268, 280, 332 and 350 nm, respectively. In addition, a significant decrease of the peak-to-valley ratio for all the bands was also observed (ESI Table S1). These changes suggested that **1** had undergone a self-assembly process in the aqueous medium.[11,20] In order to favour the assembly process and the formation of supramolecular structures through non-covalent interactions, the aqueous solution of **1** was subjected to ultrasonic treatment. The vibronic bands at 264, 274, 326 and 340 nm were red-shifted to 272, 284, 340 and 354 nm respectively as a result; a stronger bathochromic shift relative to that found without ultrasonic treatment was observed. In addition to this, $I_{326/I340}$ was found to decrease significantly from 1.33 to 0.96. These spectroscopic changes suggested that the pyrene derivative monomers had self-assembled into supramolecular structures with an offset stacking arrangement specific to J-type aggregates.[11,20-23] A sharp red-shifted band is typically expected for J-type aggregates, but several examples of broad absorption band (as observed in the present case) have been reported.[22]

In order to gain further insight into the assembly process we investigated the fluorescence properties of **1** in ethanol at 0.2, 0.4, 1, 2, 5 and 10 mM (Fig. 2a). The intensity of the monomer peak measured at 378 nm decreased upon increasing the concentration of **1**, with concomitant appearance of a new peak at 480 nm that can be safely attributed to excimer formation.[24-26]

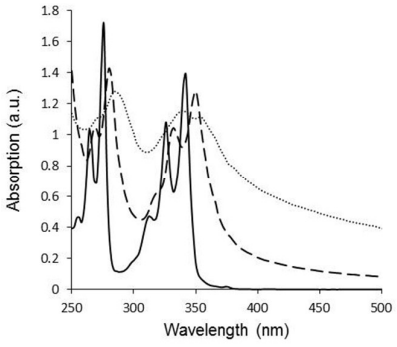

Fig. 1 UV/Vis spectra of **1** (0.1 mM) in ethanol (solid line), in water (ethanol 10 vol. %) (dashed line) and in water (ethanol 10 vol. %) after ultrasonication (dotted line).

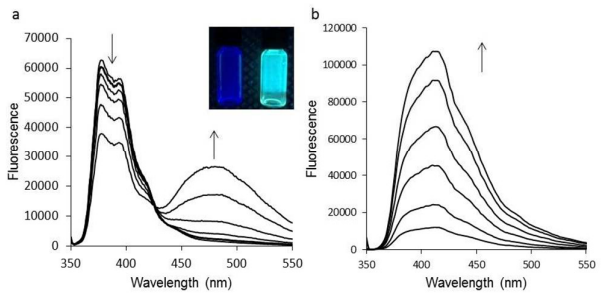

Fig. 2 Fluorescence spectra of **1** (λexc = 326 nm) in a) ethanol and in b) aqueous medium (ethanol vol. 10%) after ultrasonication at 0.2, 0.4, 1, 2, 5 and 10 mM. Inset: photo of solutions of **1** in ethanol at low concentration (left) and at high concentration (right) under UV light (λexc = 366 nm).

A significant change of the fluorescence maximum wavelength emission at low and high concentration of **1** could be observed (Fig. 2a, inset). In aqueous medium and after ultrasonic treatment, the fluorescence maximum wavelength changed to 412 nm, which corresponded to neither monomer nor excimer emission; this change is likely due to the formation of a self-assembled structure with a higher degree of structural order.

Dynamic light scattering (DLS) provided further evidence for the formation of aggregates of **1**, revealing stable colloidal objects with an average hydrodynamic diameter of 580 nm at 25°C (ESI Fig. S4). These aggregates were further analysed by field-emission scanning electron microscope (FE-SEM) and transmission electron microscope (TEM); representative micrographs are presented in Fig. 3.

The supramolecular assembly formed without ultrasonication gave a fibre-like structure (ESI Fig. S5a,b). After ultrasound treatment, well-defined linear rods with a diameter ranging from 150 nm to 500 nm and a length ranging from 1 to 3 µm were produced (Fig. 3, ESI Fig. S5c,d). These rods were stable for several months at room temperature, but higher temperatures (>40°C) promote disassembly of the supramolecular structures. Further investigations with FE-SEM allowed for the identification of smaller nanorods at the extremity of the self-assembled rods (ESI Fig. S5e,f). The size of these nanorods ranged from 15 to 35 nm, which is in the region of 9 to 21 pyrene derivative units; these nanorods exhibited a more flexible structure than the overall arrangement. Transmission electron microscopy investigations of these nanorods confirmed a high density to electrons of the entire structure, ruling out the possibility of a tube-like structure with an empty core (Fig. 3). In order to verify the integrity of **1** following self-assembly, we carried out FTIR and ^{1}H NMR analyses (ESI Fig. S6,7). Our results strongly suggested that **1** did not undergo any relevant side reaction or hydrolysis.

Slow diffusion of an ethanol solution of **1** into water over a period of ca. 10 days afforded large needle-shaped single crystals that were suitable for diffraction studies. The crystals were found to be in a monoclinic cell and structure solution was performed in the space group *Pc*. The asymmetric unit was found to contain four molecules of **1**, all of which showed disorder that was modelled at partial occupancy (Fig. 4).

View Article Online
DOI: 10.1039/C6CC09731F

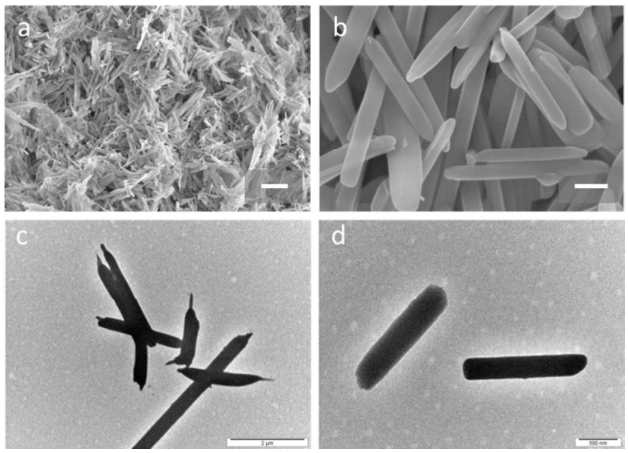

Fig. 3 FE-SEM (a, b) and TEM (e, f) micrographs of self-assembled supramolecular nanorods of pyrene derivative **1**. Scale bars represent 4 μm (a), 400 nm (b), 2 μm (c) and 500 nm (d).

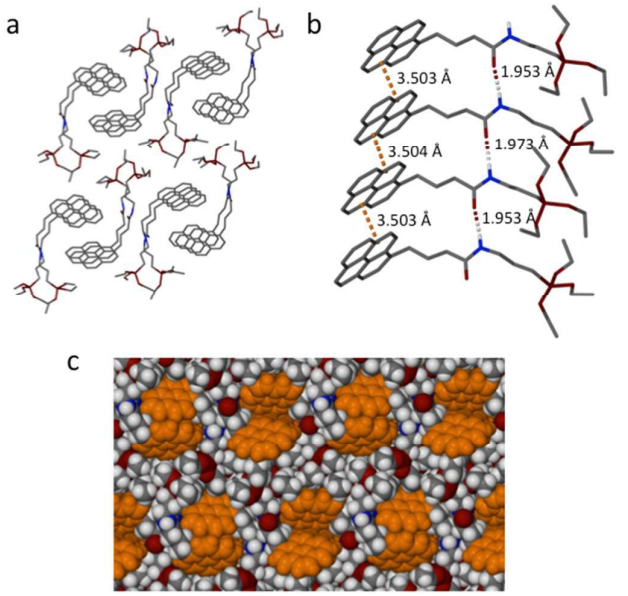

Fig. 4 Views of the single crystal X-ray structure of **1**. (a) Stick representation of the extended structure showing isolation of pyrene stacks. (b) Example of H-bonding and π-stacking interactions found between neighboring molecules of **1**. (c) Space filling representation of the extended structure. Disordered groups as well as H atoms in A and B (except for those involved in H-bonding) are omitted for clarity.‡

Examination of the extended structure showed that, as J-aggregates, the molecules are arranged in an offset stack fashion (Fig. 4). The distance separating two neighbouring pyrene derivatives units was found to be ~3.5 Å (Fig. 4b for one of the crystallographically unique stacks), whilst the angle between the pyrene planes was ~48°; the latter is below the limit of 54.7° that states the difference between J-type (θ < 54.7°) and H-type aggregates (θ > 54.7°).[22,27] Confirming the success of our molecular design, the structure also exhibits H-bonding between neighbouring donors (N-H) and acceptors (C=O) (Fig. 4b), with average N•••O and NH•••O distances of ~2.83 and ~1.99 Å respectively. Comparison of Fig. 4(a) and 4(c) further stresses the isolation of stacks within the extended structure; this is due to the arrangement of both the directing H-bonded spacers and the triethoxysilyl groups. In order to confirm bulk sample composition the supramolecular rods were also analysed by powder X-ray diffraction (ESI Fig. S8). The results show relatively good agreement between the observed powder pattern of nanorods and the calculated pattern from the single crystal of **1**. This result demonstrated the similarity of the molecular packing of **1** in the self-assembled nanorods and in the crystalline state. Crystals of **1** were found to change from colourless to orange / brown (**1***) upon exposure to sunlight over several weeks, all of which occurs with no difference in crystal morphology. Structural studies on crystals of **1*** found them to be weakly diffracting, but it was possible to obtain a data set of limited quality from which some major connectivities could be established. Crystals of **1*** were found to be in a monoclinic system and structure solution was performed in *Pc*, as was the case for **1**. Indeed, the unit cell parameters of **1*** match those of **1** very closely (ESI Table S2), providing further evidence that the crystals of **1** and **1*** are isostructural. The asymmetric unit in **1*** comprises four molecules and these are arranged in stacks as expected, but a high degree of disorder is observed in the structure; this is a potential reason for such a marked drop-off in diffraction upon moving from **1** to **1***, and is evidenced by the presence of diffuse electron density. As a result of poor diffraction and disorder in the structure the best R_1 that could be achieved was ~ 21%. In subsequent experiments we found that freshly formed crystals of **1** could be rapidly transformed to **1*** upon exposure to UV irradiation at 365 nm in just 3h (Fig. 5).

With such a marked light-induced colour change occurring, we turned to computational studies to gain insight into this irreversible solid-state process. Density functional theory (DFT): ωB97XD/aug-cc-pVDZ, and time-dependent DFT: CAM-B3LYP/aug-cc-pVDZ, were used to model the ground and excited states of two interacting pairs of pyrenes from **1** minus the silyl ether groups (2 x 2 stack of 4). The ground state optimal structure is that of a J-aggregate, an arrangement that agrees well with the one found experimentally. The TD-DFT shows a large density of states between 280-330 nm, with a significant degree of charge transfer up/down the pyrene stacks. The position of the bright states in TD-DFT agrees reasonably with the observed absorption spectra (ESI Fig. S9). Due to computational overhead geometry, optimization in the excited states was performed with smaller 6-31G* basis augmented with a diffuse set of functions on the carbons.

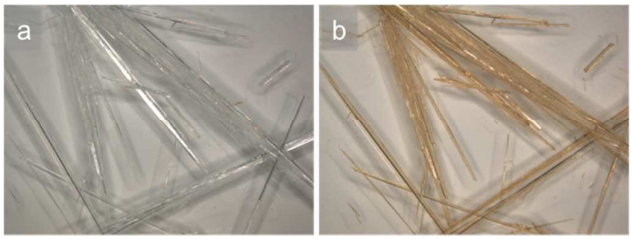

Fig. 5 Optical micrographs of crystals of **1** before and after UV_{365} irradiation for 3h.

View Article Online
DOI: 10.1039/C6CC09731F

Exploratory calculations reveal that states responsible for the CT band optimise to a similar J-aggregate but with a closing of the tilt angle between dimer pairs. We note that we did not fully optimise the displacements, rather only the gradient, but the key geometrical relaxation coordinate is indicated to be a change in the pyrene dimer angle.

As stated above, the poor quality of diffraction data precludes the ability to quantify parameters such as π-stacking/hydrogen bonding distances, angles between pyrene moieties and other structural features. Although this is the case, dissolution of orange crystals of **1*** afforded a colorless solution and ^{1}H NMR analysis confirmed that no change has been made to the molecules of **1**. All of this is suggestive that there is movement of the pyrene moieties within the stacks and that this is the origin of the drastic change in color observed upon irradiation.

To endow the nanorods with the possibility to be functionalised, a silica layer was grown on the surface of the nanorods; this was achieved through hydrolysis/condensation of the surface triethoxysilyl groups with (3-aminopropyl)-triethoxysilane and tetraethoxysilane. Polycondensation was followed by FE-SEM and confirmed effective silica layer growth on the nanorods (ESI Fig. S10). This thin layer of silica may thus be used to chemically modify the surface of the nanorods.

In summary, we have developed a strategy to produce hierarchically self-assembled nanorods of a new pyrene derivative following a template-free approach. The self-assembly process is demonstrated to first occur via π-π stacking of the molecular building block into excimers. When transferred to water, hydrogen bonding and π-π stacking interactions act synergistically to form the aggregates. Hydrophobic effects (due mainly to the pyrene moiety) likely assist the construction of the nanorods. Diffraction studies provided insight into the packing behaviour of **1** in single crystals, whilst powder X-ray diffraction confirmed the persistence of this arrangement within the nanorods. A silica layer was successfully grown on the surface of the nanorods, demonstrating the potential to functionalise these supramolecular assemblies. Finally, both single crystals and nanorods of **1** have been shown to undergo a drastic colour change upon exposure to UV light; which is likely attributable to changes in the self-assembled structures rather than chemical alteration. Work is underway to fully elucidate this phenomenon, the results of which will be reported in due course.

Notes and references

The authors declare no competing financial interests.

‡ CCDC 1483530 contains the supplementary crystallographic data for this paper. These data are provided free of charge by The Cambridge Crystallographic Data Centre.

1 C. Rest, R. Kandanelli and G. Fernandez, *Chem. Soc. Rev.*, 2015, **44**, 2543-2572.
2 E. Busseron, Y. Ruff, E. Moulin and N. Giuseppone, *Nanoscale*, 2013, **5**, 7098-7140.
3 K. E. Riley and P. Hobza, *Acc. Chem. Res.*, 2013, **46**, 927-936.
4 R. Marty, R. Nigon, D. Leite and H. Frauenrath, *J. Am. Chem. Soc.*, 2014, **136**, 3919-3927.
5 Y. Chen, B. Zhu, F. Zhang, Y. Han and Z. Bo, *Angew. Chem., Int. Ed.*, 2008, **47**, 6015-6018.
6 I. Radivojevic, I. Likhtina, X. Shi, S. Singh and C. M. Drain, *Chem. Commun.*, 2010, **46**, 1643-1645.
7 F. Würthner, *Acc. Chem. Res.*, 2016, **49**, 868-876.
8 S. Fleming and R. V. Ulijn, *Chem. Soc. Rev.*, 2014, **43**, 8150-8177.
9 F. Helmich, C. C. Lee, M. M. L. Nieuwenhuizen, J. C. Gielen, P. C. M. Christianen, A. Larsen, G. Fytas, P. E. L. G. Leclère, A. P. H. J. Schenning and E. W. Meijer, *Angew. Chem., Int. Ed.*, 2010, **49**, 3939-3942.
10 F. J. M. Hoeben, M. Wolffs, J. Zhang, S. De Feyter, P. Leclère, A. P. H. J. Schenning and E. W. Meijer, *J. Am. Chem. Soc.*, 2007, **129**, 9819-9828.
11 M. Vybornyi, A. V. Rudnev, S. M. Langenegger, T. Wandlowski, G. Calzaferri and R. Haner, *Angew. Chem., Int. Ed.*, 2013, **52**, 11488-11493.
12 A. L. Nussbaumer, D. Studer, V. L. Malinovskii and R. Häner, *Angew. Chem., Int. Ed.*, 2011, **50**, 5490-5494.
13 A. V. Rudnev, V. L. Malinovskii, A. L. Nussbaumer, A. Mishchenko, R. Häner and T. Wandlowski, *Macromolecules*, 2012, **45**, 5986-5992.
14 S. S. Babu, S. Prasanthkumar and A. Ajayaghosh, *Angew. Chem., Int. Ed.*, 2012, **51**, 1766-1776.
15 B.-Q. Ma and P. Coppens, *Chem. Commun.*, 2003, 2290-2291.
16 Z. Wang, H. Möhwald and C. Gao, *ACS Nano*, 2011, **5**, 3930-3936.
17 H. Wang, W. Zhang and C. Gao, *Biomacromolecules*, 2015, **16**, 2276-2281.
18 X. Zhang, X. Zhang, W. Shi, X. Meng, C. Lee and S. Lee, *J. Phys. Chem. B*, 2005, **109**, 18777-18780.
19 N. Kameta, M. Masuda and T. Shimizu, *Chem. Commun.*, 2015, **51**, 11104-11107.
20 H. Siu and J. Duhamel, *J. Phys. Chem. B*, 2008, **112**, 15301-15312.
21 Y. Shiki, G. Yusaku, L. Xu, K. Takashi, K. Akihide, K. Daiki, Y. Hiroko, K. Yoshihiro, S. Akinori and S. Shu, *Angew. Chem., Int. Ed.*, 2012, **51**, 6643-6647.
22 F. Würthner, T. E. Kaiser and R. S.-M. Chantu, *Angew. Chem., Int. Ed.*, 2011, **50**.
23 J. C. Xiao, Y. J. Li, Y. B. Song, L. Jiang, Y. L. Li, S. Wang, H. B. Liu, W. Xu and D. B. Zhu, *Tetrahedron Lett.*, 2007, **48**, 7599-7604.
24 T. Förster, *Angew. Chem., Int. Ed.*, 1969, **8**, 333-343.
25 L. Gai, H. Chen, B. Zou, H. Lu, G. Lai, Z. Li and Z. Shen, *Chem. Commun.*, 2012, **48**, 10721-10723.
26 Z. Xu, N. J. Singh, J. Lim, J. Pan, H. N. Kim, S. Park, K. S. Kim and J. Yoon, *J. Am. Chem. Soc.*, 2009, **131**, 15528-15533.
27 Z. An, C. Zheng, Y. Tao, R. Chen, H. Shi, T. Chen, Z. Wang, H. Li, R. Deng, X. Liu and W. Huang, *Nat. Mater.*, 2015, **14**, 685-690.